

MHPL: Minimum Happy Points Learning for Active Source Free Domain Adaptation

Fan Wang¹, Zhongyi Han¹, Zhiyan Zhang¹, Rundong He¹, Yilong Yin^{1*}

¹ School of Software, Shandong University, China

{fanwang, rundong_he}@mail.sdu.edu.cn, {hanzhongyicn, zyzhangcs}@gmail.com, ylyin@sdu.edu.cn

Abstract

Source free domain adaptation (SFDA) aims to transfer a trained source model to the unlabeled target domain without accessing the source data. However, the SFDA setting faces a performance bottleneck due to the absence of source data and target supervised information, as evidenced by the limited performance gains of the newest SFDA methods. Active source free domain adaptation (ASFDA) can break through the problem by exploring and exploiting a small set of informative samples via active learning. In this paper, we first find that those satisfying the properties of neighbor-chaotic, individual-different, and source-dissimilar are the best points to select. We define them as the minimum happy (MH) points challenging to explore with existing methods. We propose minimum happy points learning (MHPL) to explore and exploit MH points actively. We design three unique strategies: neighbor environment uncertainty, neighbor diversity relaxation, and one-shot querying, to explore the MH points. Further, to fully exploit MH points in the learning process, we design a neighbor focal loss that assigns the weighted neighbor purity to the cross entropy loss of MH points to make the model focus more on them. Extensive experiments verify that MHPL remarkably exceeds the various types of baselines and achieves significant performance gains at a small cost of labeling.

1. Introduction

Transferring a trained source model instead of the source data to the unlabeled target domain, source-free domain adaptation (SFDA) has drawn much attention recently. Since it prevents the external leakage of source data, SFDA meets privacy persevering [19, 47], data security [43], and data silos [39]. Moreover, it has important potential in many applications, *e.g.*, object detection [23], object recognition [25], and semantic segmentation [17]. However, the SFDA setting faces a performance bottleneck due to the ab-

sence of source data and target supervised information. The state-of-the-art A²Net [50] is a very powerful method that seeks a classifier and exploits classifier design to achieve adversarial domain-level alignment and contrastive category-level matching, but it only improved the mean accuracy of the pioneering work (SHOT [25]) from 71.8% to 72.8% on the challenging Office-Home dataset [45]. Although some recent studies [20, 52] utilize the transformer or mix-up to improve the performance further, they have modified the structure of the source model or changed the source data, which is not universal in privacy-preserving scenarios.

Active source free domain adaptation (ASFDA) can produce remarkable performance gains and breakthrough performance bottlenecks when a small set of informative target samples labeled by experts. Two factors must be considered to achieve significant performance gains: (1) Exploring samples that, once labeled, will improve accuracy significantly; (2) Exploiting limited active labeled target data well in adaptation. However, these two factors have not been achieved. For example, ELPT [24] uses prediction uncertainty [27] to explore active samples and applies cross-entropy loss to exploit these selected samples. While the prediction uncertainty is error-prone due to the miscalibrated source model under distribution shift [32], and the pseudo-label noise of unlabeled samples easily influence the effect of standard cross-entropy loss on active samples.

In this paper, we first find the best informative samples for ASFDA are Minimum Happy (MH) points that satisfy the properties of neighbor-chaotic, individual-different, and source-dissimilar. (1) The property of neighbor-chaotic refers to the sample's neighbor labels being very inconsistent, which measures the sample uncertainty through its environment. The Active Learning (AL) and Active DA methods, which rely on the miscalibrated model output [32] or domain discrepancy, can't identify these uncertain samples in ASFDA. As shown in Fig. 1, the samples selected by our method are more likely to fall into red blocks with label-chaotic environments than BVSB [14]. (2) The property of individual-different guarantees the diversity of selected uncertain samples to improve the effectiveness of querying.

*denotes corresponding author.

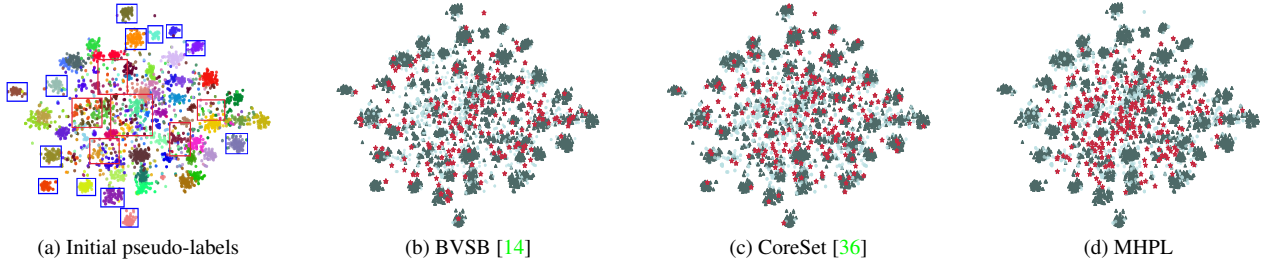


Figure 1. Feature visualization for the source model with 5% actively labeled target data on the CI→Pr task. Different colors in (a) represent different classes of pseudo-labels by clustering. Blue blocks include easily-adaptive source-similar samples with label-clean neighbors that can be learned well by SFDA methods. Red blocks include the hard-adaptive source-dissimilar samples with label-chaotic neighbors. In (b), (c), and (d), the dark green indicates that the pseudo-label is consistent with the true label, and light blue indicates the opposite. The red stars indicate the selected samples based on BVSB, CoreSet, and our MHPL.

Previous methods [32,36,38] ensure sample diversity across the global target domain. However, they would select already well-aligned source-similar samples [32] that are less informative for target adaptation as they can be learned by SFDA methods [16,44]. Fig. 1 illustrates that compared with CoreSet [36], most samples selected by our method are diverse in the source-dissimilar regions (red blocks). (3) The informative samples should be source-dissimilar, as the source-dissimilar samples are more representative of the target domain and need to be explored. Most Active DA methods [6,40] ensure source-dissimilar samples based on measuring the distribution discrepancy across domains, which is unavailable in ASFDA due to unseen source data.

Concerning the exploitation of selected samples, most methods of AL [10,34,36], Active DA [6,32,40,51], and ELPT [24] deem them as ordinary labeled samples and use standard supervised losses to learn them. However, the number of selected samples is so tiny in ASFDA that they occupy a small region of the target domain. With standard supervised losses, the model cannot be well generalized to the entire target domain, leading to poor generalization.

We propose the Minimum Happy Points Learning (MHPL) to explore and exploit the informative MH points. First, to measure the sample uncertainty, we propose a novel uncertainty metric, neighbor environment uncertainty, that is based on the purity and affinity characteristics of neighbor samples. Then, to guarantee the individual difference, we propose neighbor diversity relaxation based on performing relaxed selection among neighbors. Furthermore, the source-dissimilar characteristic of samples is maintained by our proposed one-shot querying. We select target samples at once based on the source model, as the source model without fine-tuning can better describe the distribution discrepancy across domains and the source-dissimilar samples are more likely to be explored. In addition, the selected samples are fully exploited by a new-designed neighbor focal loss, which assigns the weighted neighbor purity to the cross-entropy loss of MH points to make the model focus

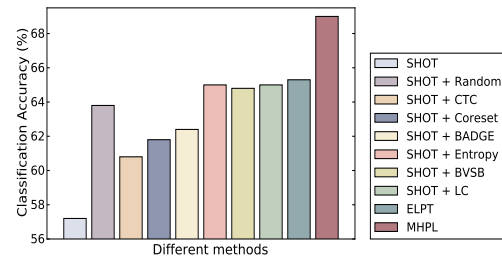


Figure 2. The comparison of ASFDA baselines (SHOT [25] + *, * denotes the active strategy), ELPT, and our MHPL with 5% active labeled target samples on Ar→CI in the Office-Home.

and learn more about them. As shown in Fig. 2, our MHPL significantly outperforms the ASFDA baselines, *i.e.*, an effective SFDA method (SHOT) + AL strategies, and the existing state-of-the-art ASFDA approach, ELPT [24].

Our contributions can be summarized as follows: (1) We discover and define the most informative active samples, Minimum Happy (MH) points for ASFDA; (2) We propose a novel MHPL framework to explore and exploit the MH points with the neighbor environment uncertainty, neighbor diversity relaxation, one-shot querying, and neighbor focal loss; (3) Extensive experiments verify that MHPL surpasses state-of-the-art methods.

2. Related Work

Domain Adaptation (DA) aims to transfer the knowledge from amounts of labeled source data to the unlabeled target domain. Most DA works attempt to align the feature distributions across domains with moment matching [28,30] or adversarial learning [7,29]. Recently, semi-supervised DA [13,15] and few-shot DA [42] have verified that utilizing a few labeled target data is helpful to performance benefits. However, the success of the above methods depends on the amount of annotated source data, which is unrealistic and unpractical in privacy-persevering scenarios.

Source Free Domain Adaptation (SFDA) has been introduced recently to relax the dependence on the source data. Existing SFDA works have made a great effort based on two categories of methods: *i.e.*, source model exploration and data generation, while they face the performance bottleneck with limited performance gains. The works based on source model exploration, SHOT [25], HCL [12], NRC [53], and A²Net [50], aim to utilize the potential distribution information in the given model. However, these methods cannot achieve strong positive transfer without more than 1% improvement over the initial SHOT [25] on Office-Home. Another line of work based on data generation, MA [22], and CPGA [33], intends to generate the source or target data to obtain supervised information, costing amounts of time and resources. But these works also perform worse as the correct samples or prototypes are difficult to generate. Hypothesis Transfer Learning (HTL) [1, 21] aims to transfer knowledge using source hypotheses and limited randomly labeled target data without the source data. However, randomly selecting target data to be labeled by experts would be inefficient. Active source free domain adaptation (ASFDA) aims to break through the performance bottleneck with a few actively labeled target data. As the first ASFDA work, ELPT [24] failed to explore and exploit informative samples, resulting in poor performance.

Active Learning (AL) aims to obtain a satisfactory model at the cost of a limited annotation budget. Existing AL methods are mainly based on two categories: (1) Uncertainty, *e.g.*, Entropy [46]; (2) Diversity, *e.g.*, CoreSet [36]. However, neither method is suitable for domain adaptation [4, 50]. Recently, most Active DA works have introduced active learning and identified active samples into domain adaptation. Utilizing a domain discriminator, AADA [40] and TQS [6] aim to explore the source-dissimilar samples. EADA [51] determines the active samples based on the discrepancy of free energy across domains. In addition, Clue [32] identifies active samples that are uncertain with high entropy and diverse in feature space. Due to domain shift and unavailable source data, it is impossible to directly apply the existing AL and Active DA criteria to ASFDA.

3. Minimum Happy Points Learning

Notation. In ASFDA, we can access a source model $h_s : \mathcal{X}_s \rightarrow \mathcal{Y}_s$ well trained on the source data and an unlabeled target domain $D_t = \{x^i\}_{i=1}^{n_t}$ from different distributions. We denote $m = \rho n_t$ as the number of selected target samples for querying, $m \ll n_t$, and ρ as the ratio of active samples. Further, we denote the small selected labeled target data by D_t^L and the unlabeled target data by D_t^U . Our method is based on a two-part network: a feature extractor f and a classifier g . The feature is denoted as $z_i = f(x_i)$. The goal of ASFDA is to obtain a satisfactory target model $h_t = g_t(f_t(x))$ with the active samples and source model.

3.1. Minimum Happy Points

We find the best informative samples for ASFDA are Minimum Happy points (MH points) that have the characteristics of neighbor-chaotic, individual-different, and source-dissimilar at the same time.

(1) **Neighbor-chaotic** samples refer to uncertain ones with label-chaotic neighbors. Meanwhile, their neighbors in a noisy environment are heavily uncertain. Annotating these samples can not only achieve self-correction but also guide the learning of their confusing neighbors, bringing significant performance gains. Further, the sample with chaotic neighbors lies potentially in the boundary of multiple classes, so learning them would promote accurate classification boundaries. Fig. 1 shows that MHPL explores more samples (red blocks) with label-chaotic neighbors than BVS [14] because BVS based solely on model uncertainty can only measure the self-uncertainty of samples.

(2) **Individual-different** samples refer to diverse ones dissimilar to each other in selected uncertain samples. MHPL can maintain local diversity based on uncertain samples that is better than the global diversity as Coreset does. Because Coreset would explore already well-aligned source-similar samples or worthless outliers, while MHPL does not (see Fig. 1).

(3) **Source-dissimilar** samples refer to those that are biased toward the target distribution. Following the covariate shift assumption [5], the target data D_t can be divided into easily-adaptive source-similar instances D_t^s and hard-adaptive source-dissimilar instances D_t^t . Selecting samples from D_t^s would lead to limited performance gains on the target domain since SFDA methods already learn D_t^s [16, 44]. As shown in Fig. 1, the samples selected by BVS have more chances to fall in the regions of source-similar samples (blue blocks), while the samples selected by our MHPL are mostly source-dissimilar (red blocks).

3.2. Minimum Happy Points Exploration

As shown in Fig. 3, we propose the neighbor environment uncertainty, neighbor diversity relaxation, and one-shot querying to explore the MH points.

Neighbor Environment Uncertainty. Instead of relying heavily on the self-uncertainty of target samples, the neighbor environment uncertainty evaluates target sample uncertainty by measuring the neighbor environments they are in. Given a target sample x , its neighbor environment uncertainty NEU(x) is defined by multiplying the neighbor purity NP(x) and the neighbor affinity NA(x):

$$\text{NEU}(x) = \text{NP}(x) * \text{NA}(x). \quad (1)$$

Note that $\text{NP}(x) \geq 0$ and $0 \leq \text{NA}(x) \leq 1$. A sample with a high value of NEU would have noisy and close neighbors, satisfying the neighbor-chaotic characteristic of MH points.

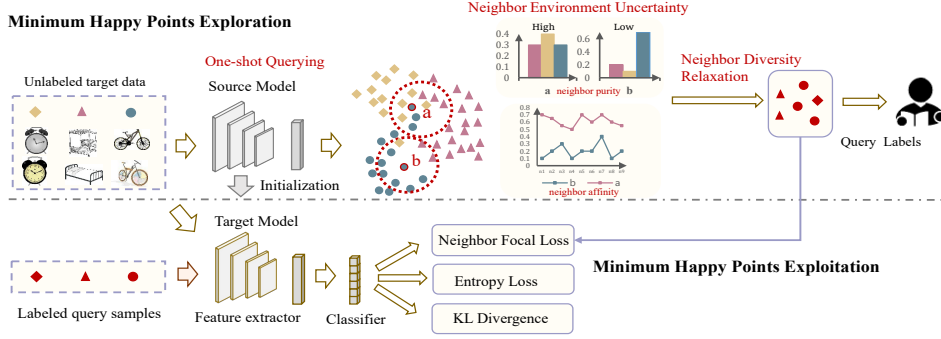


Figure 3. The framework of Minimum Happy Points Learning (MHPL). The informative active samples are explored by neighbor environment uncertainty, neighbor diversity relaxation and one-shot querying, and then are exploited by our neighbor focal loss.

Next, we first define the concept of neighbor and then introduce the neighbor purity and the neighbor affinity, orderly.

Based on the feature space $\mathcal{F} = \{z_1, z_2, \dots, z_{n_t}\}$ of target data and the cosine similarity measurement [25], we define the samples that are close to x in the feature space as the neighbors of x :

$$S_N(x) = \{N_1, \dots, N_q\}, \text{ and } S_N^Y(x) = \{Y_{N_1}, \dots, Y_{N_q}\}, \quad (2)$$

where q denotes the number of neighbors, S_N represents the neighbor sample space of x , and S_N^Y represents the neighbor pseudo-label space of x . The pseudo-labels of samples are obtained by deep clustering [25]. Y_{N_q} denotes the pseudo-label of the neighbor sample N_q .

Intuitively, if the neighbor labels of a sample are not consistent and the distance between the sample and its neighbors is very close in the feature space, the sample that seems to violate the clustering assumption [55] would have great uncertainty. Based on this intuitive insight, we design the neighbor purity and neighbor affinity as follows.

Neighbor purity describes the chaotic degree of neighbor labels around a sample. For calculating the neighbor purity $NP(x)$, we first establish the neighbor class probability distribution space $S_N^p(x)$:

$$S_N^p(x) = \{p_1, \dots, p_k\}, \quad (3)$$

where p_k represents the proportion of samples labeled as class k in q neighbors. Take samples a and b in Fig. 3 as examples, $S_N^p(a) = \{0.3, 0.4, 0.3\}$, $S_N^p(b) = \{0.2, 0.1, 0.7\}$.

Then the neighbor purity of sample x is measured by the neighbor entropy:

$$NP(x) = -\sum_{k=1}^K p_k \log p_k, \text{ s.t. } p_k \in S_N^p(x). \quad (4)$$

The sample with a high value of NP has label-noisy neighbors, and such a sample is more likely to be identified and selected as an uncertain one.

Neighbor affinity describes how close a sample is to its neighbors. To measure the degree of affinity, we first define the neighbor similarity space S_N^s for each sample by

$$S_N^s(x) = \{S_{N_1}, \dots, S_{N_q}\}, \quad (5)$$

where S_{N_1} represents the cosine similarity between x and its neighbor N_1 . Further, the neighbor affinity is measured by the average similarity between x and its neighbors:

$$NA(x) = \frac{S_{N_1} + \dots + S_{N_q}}{q}, \text{ s.t. } S_{N_q} \in S_N^s(x). \quad (6)$$

The lower the neighbor affinity, the further the sample to its neighbors. Utilizing NA, the samples selected are less likely to be outliers. Meanwhile, the sample has noisy and close neighbors with considerable uncertainty. Taking Fig. 3 as an example, the sample a is more likely to be selected as a neighbor-chaotic MH point.

The advantages of NEU are two-fold. Firstly, previous SFDA works [53, 54] have proved that the target samples' deep features extracted by the source model can still form clean clusters under domain shift to a certain extent. Fig. 1 shows the visualization of target features and further verifies this phenomenon. Different from SFDA methods [53, 54] that encourage neighbor label consistency, NEU measures the sample uncertainty from the neighbor label inconsistency, which would be better than the strategies that rely solely on the miscalibrated uncertainty of model predictions. Secondly, NEU has the advantages of ensemble learning [55] and lets numerous neighbor crowds calibrate the individual uncertainty and improve the fault tolerance of target sample selection.

Neighbor Diversity Relaxation. In contrast to existing methods [32, 38] that maintain sample diversity globally and may select the source-similar and uninformative samples, neighbor diversity relaxation (NDR) guarantees individual differences in neighbor-chaotic samples locally. In particular, NDR performs neighbor relaxation on candidate samples with high neighbor environment uncertainty. The main

Algorithm 1 Neighbor Diversity Relaxation.

Require: $D_t^L = \emptyset, D_t, m,$ and o ;

- 1: Sort the samples in D_t in reverse order by the value of NEU, and let $i = 0$;
 - 2: **while** $\text{length}(D_t^L) \leq m$ **do**
 - 3: Select the candidate sample x_i and obtain its nearest neighbor set $S_N(x_i)^o$,
 - 4: **if** $S_N(x_i)^o \cap D_t^L = \emptyset$ **then** $D_t^L \leftarrow x_i$,
 - 5: **else** Skip the selection of sample x_i ,
 - 6: **end while**
-

procedure of NDR is shown in algorithm 1. For a candidate sample x_i with a high $\text{NEU}(x_i)$, we first evaluate its nearest set of neighbors $S_N(x_i)^o$ (o denotes the number of neighbors) before putting it in D_t^L . If any neighbor in the $S_N(x_i)^o$ has been put in the D_t^L , then x_i has no chance of being selected for expert annotation. Thus, redundant samples with similar features would have few chances to be chosen, ensuring diversity in neighbor-chaotic samples.

One-shot Querying. In order to explore source-dissimilar samples, we perform one-shot querying, selecting samples at once according to the raw source model. The reasons are two-fold. For one thing, without the source data, we can measure the domain discrepancy by observing how the target data behaves on the source model, as the source model without fine-tuning can better describe the distribution discrepancy across domains. The samples that can be easily classified by the source model are commonly source-similar instances, which mainly occur in label-clean clusters [41, 53]. Otherwise, the samples with label-chaotic neighbors are severely misclassified and source-dissimilar instances, which can be effectively explored by our proposed criterion. For another, as the training model is gradually biased toward the target domain, it is difficult to determine if the samples are source-similar or source-dissimilar.

3.3. Minimum Happy Points Exploitation

Neighbor Focal Loss is designed to make the model focus more on informative MH points to ensure the generalization of the target domain. NF loss is inspired by, but not the same as focal loss [26]. For one side, focal loss aims to alleviate the overfitting problem of cross-entropy loss for imbalanced object detection datasets, while NF loss is proposed to exploit the MH points thoroughly. For another, focal loss assigns the weights from the miscalibrated model’s beliefs to hard samples, while NF loss assigns the neighbor purity and a larger weight α to the MH points:

$$L_{NF}(h_t; \mathcal{D}_t^L) = -\mathbb{E}_{x \in \mathcal{D}_t^L} \sum_{k=1}^K \alpha \text{NP}(x) l_k \log(\delta_k(h_t(x))), \quad (7)$$

where $\delta_k(\mathbf{b}) = \frac{\exp(\mathbf{b}_k)}{\sum_i \exp(\mathbf{b}_i)}$ denotes the k -th element in the softmax output of a K -dimensional vector \mathbf{b} , and l_k is ‘1’

Algorithm 2 Minimum Happy Points Learning.

Require: source model h_s , target data D_t , labeled target set $D_t^L = \emptyset$, maximum number of epochs E , trade-off parameters α, β, m ;

- 1: Initialize the target model h_t with h_s and obtain pseudo-labels of target data based clustering;
 - 2: $\forall x \in D_t$, compute $\text{NP}(x)$ and $\text{NA}(x)$ to serve as $\text{NEU}(x)$ with Eq. (1 - 6);
 - 3: $D_t^L \leftarrow$ select m samples with NEU and algorithm 1;
 - 4: Let epoch = 1, iter_num = 0;
 - 5: **while** epoch $\leq E$ **do**
 - 6: Obtain pseudo-labels of D_t^U from deep clustering;
 - 7: **while** iter_num $< n_b$ **do**
 - 8: Calculate neighbor focal loss, entropy loss and KL divergence with Eq. (7 - 10);
 - 9: Update model h_t with Eq. (11).
 - 10: **end while**
 - 11: **end while**
-

for the correct class and ‘0’ for the rest.

Meanwhile, the NF loss assigns a smaller weight β to the rest target samples D_t^U . NF loss uses their pseudo-labels from clustering and makes the model not tilt toward them during training:

$$L_{NF}(h_t; \mathcal{D}_t^U) = -\mathbb{E}_{x \in \mathcal{D}_t^U} \sum_{k=1}^K \beta l_k \log(\delta_k(h_t(x))). \quad (8)$$

In summary, NF loss is defined as:

$$L_{NF}(h_t; \mathcal{D}_t) = L_{NF}(h_t; \mathcal{D}_t^L) + L_{NF}(h_t; \mathcal{D}_t^U). \quad (9)$$

For one thing, NF loss utilizes all the target data and prevents learning active samples from being influenced by samples with wrong pseudo-labels, ensuring the target domain’s generalization. For another, assigning neighbor purity could penalize the mistakes on MH points that are more important than ordinary samples for generalization.

Entropy loss and KL divergence are introduced to guarantee the unambiguous and balanced classes [3, 11], which has been widely used in clustering [8, 18], and several DA works [12, 25, 37, 41, 48, 49]:

$$L_{ent}(h_t; \mathcal{D}_t) = -\mathbb{E}_{x \in \mathcal{D}_t} \sum_{k=1}^K \delta_k(h_t(x)) \log(\delta_k(h_t(x))),$$

$$L_{div}(h_t; \mathcal{D}_t) = -\mathbb{E}_{x \in \mathcal{D}_t} \sum_{k=1}^K \text{KL}(\hat{p}_k || q_k), \quad (10)$$

where $q_{\{k=1, \dots, K\}} = \frac{1}{K}$, $\hat{p}_k = \frac{1}{n_t} \sum \delta(h_t(x))^{(k)}$ is the mean prediction of the k -th target data.

Overall, the final objective can be stated as

$$L = L_{NF}(h_t; \mathcal{D}_t) + L_{ent}(h_t; \mathcal{D}_t) + L_{div}(h_t; \mathcal{D}_t). \quad (11)$$

To conclude, the workflow of MHPL is illustrated in Algorithm 2.

Table 1. Accuracy (%) on Office-Home (ResNet50) under different settings with 5% labeled target samples ("SF" in tables denotes source data free, *i.e.*, adaptation without source data).

Categories	Method	SF	Ar→Cl	Ar→Pr	Ar→Re	Cl→Ar	Cl→Pr	Cl→Re	Pr→Ar	Pr→Cl	Pr→Re	Re→Ar	Re→Cl	Re→Pr	Avg
None	Source-only	✓	45.5	68.4	75.2	53.4	63.7	65.6	52.4	41.0	73.6	65.9	46.3	78.2	60.8
SFDA	CPGA [33]	✓	59.3	78.1	79.8	65.4	75.5	76.4	65.7	58.0	81.0	72.0	64.4	83.3	71.6
	SHOT [25]	✓	57.1	78.1	81.5	68.0	78.2	78.1	67.4	54.9	82.2	73.3	58.8	84.3	71.8
	NRC [53]	✓	57.7	80.3	82.0	68.1	79.8	78.6	65.3	56.4	83.0	71.0	58.6	85.6	72.2
	A ² Net [50]	✓	58.4	79.0	82.4	67.5	79.3	78.9	68.0	56.2	82.9	74.1	60.5	85.0	72.8
Active DA	AADA [40]	×	56.6	78.1	79.0	58.5	72.7	71.0	60.1	53.1	77.0	70.6	57.0	84.5	68.3
	TQS [6]	×	58.6	81.1	81.5	61.1	76.1	73.3	61.2	54.7	79.7	73.4	58.9	86.3	72.5
	Clue [32]	×	58.0	79.3	80.9	68.8	77.5	76.7	66.3	57.9	81.4	75.6	60.8	86.3	72.5
	EADA [51]	×	63.6	84.4	83.5	70.7	83.7	80.5	73.0	63.5	85.2	79.4	65.4	88.6	76.7
ASFDA	Base	✓	57.2	78.5	81.5	68.5	79.1	78.6	67.5	56.3	82.2	73.7	58.5	83.6	72.1
	Random	✓	63.8	81.4	83.9	71.3	82.2	81.4	68.8	62.4	83.3	76.1	63.8	85.8	75.2
	CTC	✓	60.8	78.7	82.2	69.3	79.2	79.8	68.6	59.4	82.2	74.6	61.7	84.4	73.4
	CoreSet [36]	✓	61.8	81.8	83.3	71.1	82.9	81.6	70.7	60.5	84.7	76.1	61.7	86.1	75.2
	BADGE [2]	✓	62.4	82.7	83.9	71.5	83.0	81.8	71.2	62.7	84.6	76.2	62.9	87.8	75.9
	Entropy [46]	✓	65.0	84.0	85.9	71.8	83.8	82.6	70.7	63.8	85.1	77.8	64.1	88.1	76.9
	BVSB [14]	✓	64.8	84.4	85.5	72.0	83.2	83.4	70.4	63.9	85.0	77.5	65.0	88.1	76.9
	LC [10]	✓	65.0	84.0	85.4	72.1	83.0	82.8	71.0	64.9	85.1	78.0	64.8	87.9	77.0
	ELPT [24]	✓	65.3	84.1	84.9	72.9	84.4	82.8	69.8	63.3	86.1	76.2	65.6	89.1	77.0
	MHPL	✓	69.0	85.7	86.4	72.6	87.4	84.2	73.3	67.4	86.4	80.1	69.6	89.8	79.3

4. Experiments

Benchmarks. We adopt three benchmark datasets. Office-31 [35] is a small-scale DA dataset with 31 classes and 3 domains: Amazon, Dslr, and Webcom. Office-Home [45] is a more challenging DA dataset with 65 classes and 4 domains: Artistic images, Clip Art images, Product images, and Real-world images. VisDA-2017 [31] is a large simulation-to-real dataset with 12 classes, its source domain consists of 152 thousand images and its target domain has 55 thousand real images.

Baselines. We construct four types of methods as baselines. (i) Source free domain adaptation: SHOT [25], MA [22], HCL [12], CPGA [33], NRC [53], and A²Net [50]. (ii) Active learning: (1) **Random**: random samples. (2) **Entropy** [46]: samples with highest entropy. (3) **BVSB** [14]: samples with the smallest difference between top-2 class probabilities. (4) **LC** (least confidence) [10]: samples with smallest probability. (5) **CoreSet** [36]: samples selected by a set-cover problem. (6) **CTC**: samples that are closest to clustering centers. (7) **BADGE** [2]: construct diverse batches by running KMeans++, incorporating model uncertainty and diversity. (iii) Active DA: **AADA** [40], **TQS** [6], **CLUE** [32], and **EADA** [51]. (iv) ASFDA: ELPT [24].

Implementation. We report the main results upon the backbone of ResNet-50 [9] for Office-Home and Office-31, as well as ResNet-101 for VisDA-2017. We adopt the same network architecture as SHOT [25]. We conduct SGD with momentum 0.9 and batch size of 64 for all datasets. The learning rate is set to 1e-2 for Office-31 and Office-Home, and 1e-3 for VisDA-2017. For the number of neighbors q , we set nine for Office-31, twenty for Office-Home, and five for VisDA-2017. Further, we set $\alpha = 3$, $\beta = 0.3$, and $o = 5$ for all datasets. More implementation details, full results on other backbones, and sensitivity analysis on the hyper-

parameters are added in the supplementary materials.

4.1. Main Results

Results on object recognition. Our method MHPL significantly outperforms existing SFDA methods, successfully breaking through the performance bottleneck of SFDA with limited annotations. Firstly, MHPL achieves state-of-the-art in the ASFDA setting. As shown in Table 1, MHPL surpasses on average by 6.5% over the state-of-the-art SFDA method A²Net on Office-Home with only 5% of labeled target data. Especially in challenging tasks, MHPL achieves significant improvements, *e.g.*, the accuracy of MHPL is 10.6% and 11.2% higher than that of A²Net on tasks Ar→Cl and Pr→Cl, respectively. As shown in Table 2, the accuracy of MHPL also remarkably outperforms all SFDA baselines on VisDA-2017 and Office-31. Secondly, MHPL can better explore and exploit MH points and maximize the performance gains compared to existing active strategies, and ELPT [24]. As shown in Tables 1, 2, MHPL outperforms all ASFDA baselines on most challenging tasks. Finally, as shown in Tables 1, 2, 3, it is fascinating that MHPL can outperform all active domain adaptation methods without accessing the source data. In light of this phenomenon, instead of focusing on the source-similar samples that can be easily learned, exploring the distribution of source-dissimilar MH points in the target domain might be more effective, thus further enhancing the generalization performance of the target model.

4.2. Analysis

Comparison of MH points and LC points. To further analyze the effectiveness of MH points, we compare the performance gains when fine-tuning the target model with MH points and LC points selected using the state-of-the-

Table 2. Accuracy (%) on VisDA-2017 (ResNet-101) and Office-31 (ResNet-50) with 5% labeled target samples ("SF" in tables denotes source data free, *i.e.*, adaptation without source data).

Categories	Method	SF	VisD A-2017	A→D	A→W	D→A	D→W	W→A	W→D	Avg
None	Source-only	✓	50.0	79.3	76.6	60.5	96.6	63.8	98.8	79.3
SFDA	SHOT [25]	✓	82.4	94.0	90.1	74.7	98.4	74.3	99.9	88.6
	CPGA [33]	✓	86.0	94.4	94.1	76.0	98.4	76.6	99.8	89.9
	HCL [12]	✓	83.5	90.8	91.3	72.7	98.2	72.7	100.0	87.6
	NRC [53]	✓	85.9	96.0	90.8	75.3	99.0	75.0	100.0	89.4
	A ² Net [50]	✓	84.3	94.5	94.0	76.7	99.2	76.1	100.0	90.1
Active DA	AADA [40]	×	-	89.2	87.3	78.2	99.5	78.7	100.0	88.8
	TQS [6]	×	-	92.8	92.2	80.6	100.0	80.4	100.0	91.1
	Clue [32]	×	-	92.0	87.3	79.0	99.2	79.6	99.8	89.5
	EADA [51]	×	-	97.7	96.6	82.1	100.0	82.8	100.0	93.2
ASFDA	Base	✓	83.3	93.8	91.5	76.0	99.0	74.7	100.0	89.2
	Random	✓	85.1	94.0	94.7	77.7	98.9	77.6	100.0	90.5
	CTC	✓	84.0	93.8	90.8	77.3	99.0	76.2	100.0	89.5
	CoreSet [36]	✓	85.9	93.4	92.5	78.4	99.1	78.2	100.0	90.3
	BADGE [2]	✓	86.0	94.2	93.5	79.2	99.1	79.2	100.0	90.9
	Entropy [46]	✓	86.7	95.6	95.4	80.3	99.1	80.1	100.0	91.8
	BVSB [14]	✓	86.5	96.4	95.7	79.2	99.1	80.5	100.0	91.9
	LC [10]	✓	86.7	95.6	95.4	80.0	99.1	80.6	100.0	91.8
	ELPT [24]	✓	89.2	98.0	97.2	81.2	99.4	80.7	100.0	92.8
	MHPL	✓	91.3	97.8	96.7	82.5	99.3	82.6	100.0	93.2

Table 3. Accuracy (%) on VisDA-2017 (ResNet-50) with 5% labeled target samples.

Method	AADA [40]	TQS [6]	Clue [32]	EADA [51]	MHPL
Acc (%)	80.8 ± 0.4	83.1 ± 0.4	85.2 ± 0.4	88.3 ± 0.1	89.6 ± 0.1

art LC [10] in several challenging tasks on Office-Home. As shown in Table 4, identifying 5% of active samples and labeling them greatly improves the source models with different networks. Furthermore, MH points selected by our method provide more information than LC points and guarantee better generalization to the target domain.

Table 4. Accuracy (%) on challenging tasks under different networks with 5% labeled target samples on Office-home.

Networks	active samples	Ar→Cl	Cl→Ar	Cl→Pr	Pr→Cl	Avg
VGG16	Source-only	35.2	48.0	60.5	35.4	44.8
	LC points	46.2	62.1	75.7	48.4	58.1
	MH Points	49.6	63.0	78.0	50.4	60.3
ResNet50	Source-only	45.5	53.4	63.7	46.3	52.2
	LC points	58.7	69.0	80.7	60.9	67.3
	MH Points	60.3	69.9	83.8	61.9	69.0

Ablation analysis. To investigate the efficacy of key components of our criterion for selecting minimum happy points, we firstly conduct an ablation study with the following variants on Ar→Cl in various sample selection ratios from 1% to 10%: (i) MHPL w/o NEU (all sample uncertainties are randomly assigned); (ii) MHPL w/o NDR; (iii) MHPL w/o OSQ (one-shot querying, the samples are selected in the fifth epoch of model training). As shown in Fig. 4(a), the entire method outperforms other variants in various selection ratios, indicating the necessity of each key component. Especially when the ratio of active samples is larger, the performance improvement of their combination is more obvious. Next, we analyze each of them in detail.

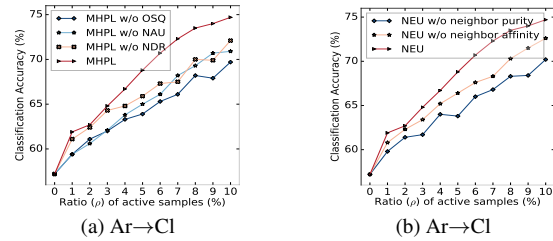


Figure 4. Ablation study on key components of MHPL and NEU at different selection ratios.

- **Neighbor environment uncertainty (NEU).** We conduct an ablation study to verify the effectiveness of neighbor purity and neighbor affinity in NEU. As shown in Fig. 4(b), MHPL with NEU performs better than its individual parts in various selection ratios.
- **Neighbor diversity relaxation (NDR).** As shown in Fig. 5, the samples selected with NDR have more diversity among the high overlapping regions.
- **One-shot querying (OSQ).** To verify the effectiveness of one-shot querying, we compare the effect with samples selected at different epochs of model training. As shown in Fig. 6(a), the abscissa indicates the epoch of model training for sample selection, where epoch zero represents the source model. It is observed that the samples selected by the source model obtain larger model performance gains on Ar→Cl. Additionally, when sample selection is made on larger epochs,

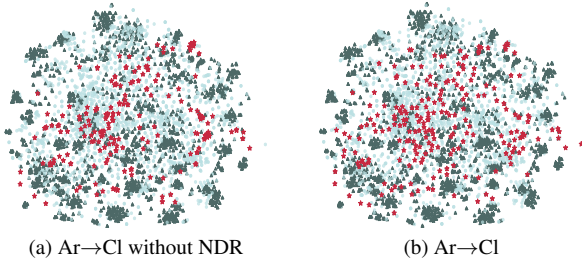


Figure 5. T-SNE visualization of representations with and without NDR in Ar→Cl on Office-Home.

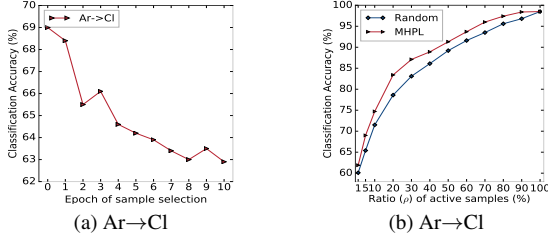


Figure 6. Ablation study on OSQ and random selection.

the model performance is significantly degraded, as the trained model cannot correctly reflect the distribution discrepancy, resulting in difficulty exploring the source-dissimilar samples.

Effect of MH points. Given that MHPL is based on strong information maximization loss [25] and new proposed neighbor focal loss, we conduct a necessary experiment: replace the MH points with randomly selected samples of equal amount in all objective Eq. (9 - 11) on Ar→Cl. As shown in Fig. 6(b), the model gains brought from MH points are always much higher than random samples.

Effect on learning neighbors. In addition, we evaluate the role of selected samples in learning their neighbors’ pseudo-labels using MHPL and state-of-the-art LC [10]. Fig. 7 shows the accuracy of the selected sample’s initial neighbors before (dark color) and after training (light color). After training, the accuracy of initial neighbors improves more significantly than it did before training, demonstrating that selected samples have better guidance on their confusing neighbors. The lighter the color, the better the performance. It is obvious that MHPL is better at exploring neighbors than LC in all tasks, especially in challenging tasks Ar→Cl, Pr→Cl, and Re→Cl.

Ablation on loss functions. To demonstrate the effect of loss functions in Eq. (11), we perform ablation studies on Ar→Cl at various sample selection ratios. As shown in Fig. 8(a), the effect of NF loss increases as more active samples are chosen. Meanwhile, entropy loss and KL divergence also promote model learning. After removing NF loss (yellow), the accuracy of different selection ratios remains

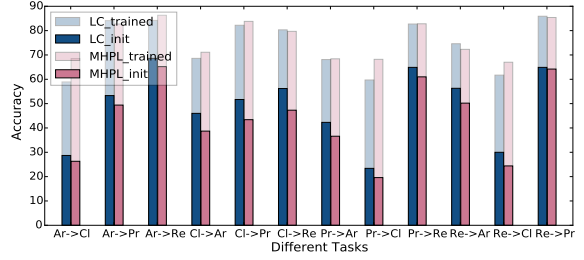


Figure 7. Mean accuracy of initial neighbors before and after training on Office-Home.

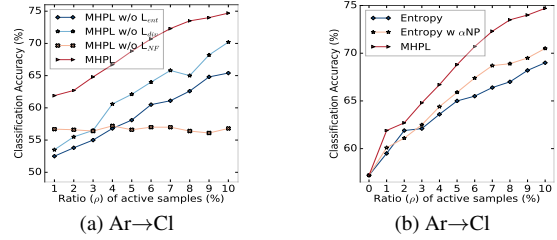


Figure 8. Ablation studies on loss functions.

the same because the selected samples do not participate in training, and the model is always trained using entropy loss and KL divergence. To verify the versatility of NF loss, we integrate it into other sample selection strategies. For instance, we assign the weight, αNP , to the samples selected by entropy [10], and the value of NP is calculated by entropy [46]. As shown in Fig. 8(b), the accuracy with αNP (green) is always better than entropy with standard cross-entropy loss (blue) on Ar→Cl, while their results are still lower than our MHPL (red).

5. Conclusion

This paper investigates the active source free domain adaptation (ASFDA), which can break through the performance bottleneck of SFDA with the minimum cost of data annotation in privacy-preserving scenarios. We first find that the samples that satisfy the properties of neighbor-chaotic, individual-different, and source-dissimilar are the most informative samples and define them as the minimum happy (MH) points, but the existing methods are difficult to explore and exploit them. We then design the minimum happy points learning to explore and exploit the MH points well and improve the model performance effectively.

Acknowledgment

This work is supported by the National Natural Science Foundation of China (62176139), the Major Basic Research Project of Natural Science Foundation of Shandong Province (ZR2021ZD15), the Young Elite Scientists Sponsorship Program by CAST.

References

- [1] Sk Miraj Ahmed, Aske R Lejbolle, Rameswar Panda, and Amit K Roy-Chowdhury. Camera on-boarding for person re-identification using hypothesis transfer learning. In *Proceedings of the IEEE/CVF Conference on Computer Vision and Pattern Recognition*, pages 12144–12153, 2020. [3](#)
- [2] Jordan T Ash, Chicheng Zhang, Akshay Krishnamurthy, John Langford, and Alekh Agarwal. Deep batch active learning by diverse, uncertain gradient lower bounds. *arXiv preprint arXiv:1906.03671*, 2019. [6](#), [7](#)
- [3] John Bridle, Anthony Heading, and David MacKay. Unsupervised classifiers, mutual information and phantom targets. *Advances in neural information processing systems*, 4, 1991. [5](#)
- [4] Chu. Denoised maximum classifier discrepancy for source-free unsupervised domain adaptation. In *Thirty-Sixth AAAI Conference on Artificial Intelligence (AAAI-22)*, volume 2, 2022. [3](#)
- [5] Shai Ben David, Tyler Lu, Teresa Luu, and Dávid Pál. Impossibility theorems for domain adaptation. In *Proceedings of the Thirteenth International Conference on Artificial Intelligence and Statistics*, pages 129–136. JMLR Workshop and Conference Proceedings, 2010. [3](#)
- [6] Bo Fu, Zhangjie Cao, Jianmin Wang, and Mingsheng Long. Transferable query selection for active domain adaptation. In *IEEE Conference on Computer Vision and Pattern Recognition, CVPR 2021, virtual, June 19-25, 2021*, pages 7272–7281. Computer Vision Foundation / IEEE, 2021. [2](#), [3](#), [6](#), [7](#)
- [7] Yaroslav Ganin and Victor Lempitsky. Unsupervised domain adaptation by backpropagation. In *International conference on machine learning*, pages 1180–1189. PMLR, 2015. [2](#)
- [8] Kamran Ghasedi Dizaji, Amirhossein Herandi, Cheng Deng, Weidong Cai, and Heng Huang. Deep clustering via joint convolutional autoencoder embedding and relative entropy minimization. In *Proceedings of the IEEE international conference on computer vision*, pages 5736–5745, 2017. [5](#)
- [9] Kaiming He, Xiangyu Zhang, Shaoqing Ren, and Jian Sun. Deep residual learning for image recognition. In *Proceedings of the IEEE conference on computer vision and pattern recognition*, pages 770–778, 2016. [6](#)
- [10] Tao He, Xiaoming Jin, Guiguang Ding, Lan Yi, and Chenggang Yan. Towards better uncertainty sampling: Active learning with multiple views for deep convolutional neural network. In *2019 IEEE International Conference on Multimedia and Expo (ICME)*, pages 1360–1365. IEEE, 2019. [2](#), [6](#), [7](#), [8](#)
- [11] Weihua Hu, Takeru Miyato, Seiya Tokui, Eiichi Matsumoto, and Masashi Sugiyama. Learning discrete representations via information maximizing self-augmented training. In *International conference on machine learning*, pages 1558–1567. PMLR, 2017. [5](#)
- [12] Jiaying Huang, Dayan Guan, Aoran Xiao, and Shijian Lu. Model adaptation: Historical contrastive learning for unsupervised domain adaptation without source data. *Advances in Neural Information Processing Systems*, 34, 2021. [3](#), [5](#), [6](#), [7](#)
- [13] Pin Jiang, Aming Wu, Yahong Han, Yunfeng Shao, Meiyu Qi, and Bingshuai Li. Bidirectional adversarial training for semi-supervised domain adaptation. In *IJCAI*, pages 934–940, 2020. [2](#)
- [14] Ajay J. Joshi. Multi-class active learning for image classification. In *2009 IEEE Computer Society Conference on Computer Vision and Pattern Recognition (CVPR 2009), 20-25 June 2009, Miami, Florida, USA*, pages 2372–2379. IEEE Computer Society, 2009. [1](#), [2](#), [3](#), [6](#), [7](#)
- [15] Taekyung Kim and Changick Kim. Attract, perturb, and explore: Learning a feature alignment network for semi-supervised domain adaptation. In *European conference on computer vision*, pages 591–607. Springer, 2020. [2](#)
- [16] Youngeun Kim, Donghyeon Cho, Priyadarshini Panda, and Sungeun Hong. Progressive domain adaptation from a source pre-trained model. *arXiv preprint arXiv:2007.01524*, 2020. [2](#), [3](#)
- [17] Marvin Klingner, Jan-Aike Termöhlen, Jacob Ritterbach, and Tim Fingscheidt. Unsupervised batchnorm adaptation (UBNA): A domain adaptation method for semantic segmentation without using source domain representations. In *IEEE/CVF Winter Conference on Applications of Computer Vision Workshops, WACV - Workshops, Waikoloa, HI, USA, January 4-8, 2022*, pages 210–220. IEEE, 2022. [1](#)
- [18] Andreas Krause, Pietro Perona, and Ryan Gomes. Discriminative clustering by regularized information maximization. *Advances in neural information processing systems*, 23, 2010. [5](#)
- [19] Inda Kreso, Amra Kapo, and Lejla Turulja. Data mining privacy preserving: Research agenda. *Wiley Interdisciplinary Reviews: Data Mining and Knowledge Discovery*, 11(1):e1392, 2021. [1](#)
- [20] Jogendra Nath Kundu, Akshay R. Kulkarni, Suvaansh Bhambri, Deepesh Mehta, Shreyas Anand Kulkarni, Varun Jampani, and Venkatesh Babu Radhakrishnan. Balancing discriminability and transferability for source-free domain adaptation. In Kamalika Chaudhuri, Stefanie Jegelka, Le Song, Csaba Szepesvári, Gang Niu, and Sivan Sabato, editors, *International Conference on Machine Learning, ICML 2022, 17-23 July 2022, Baltimore, Maryland, USA*, volume 162 of *Proceedings of Machine Learning Research*, pages 11710–11728. PMLR, 2022. [1](#)
- [21] Ilja Kuzborskij and Francesco Orabona. Stability and hypothesis transfer learning. In *International Conference on Machine Learning*, pages 942–950. PMLR, 2013. [3](#)
- [22] Rui Li, Qianfen Jiao, Wenming Cao, Hau-San Wong, and Si Wu. Model adaptation: Unsupervised domain adaptation without source data. In *Proceedings of the IEEE/CVF Conference on Computer Vision and Pattern Recognition*, pages 9641–9650, 2020. [3](#), [6](#)
- [23] Xianfeng Li, Weijie Chen, Di Xie, Shicai Yang, Peng Yuan, Shiliang Pu, and Yueting Zhuang. A free lunch for unsupervised domain adaptive object detection without source data. In *Thirty-Fifth AAAI Conference on Artificial Intelligence, AAAI 2021, Thirty-Third Conference on Innovative Applications of Artificial Intelligence, IAAI 2021, The Eleventh Symposium on Educational Advances in Artificial Intelligence*,

- EAAI 2021, Virtual Event, February 2-9, 2021, pages 8474–8481. AAAI Press, 2021. [1](#)
- [24] Xinyao Li, Zhekai Du, Jingjing Li, Lei Zhu, and Ke Lu. Source-free active domain adaptation via energy-based locality preserving transfer. In *Proceedings of the 30th ACM International Conference on Multimedia*, pages 5802–5810, 2022. [1](#), [2](#), [3](#), [6](#), [7](#)
- [25] Jian Liang, Dapeng Hu, and Jiashi Feng. Do we really need to access the source data? source hypothesis transfer for unsupervised domain adaptation. In *International Conference on Machine Learning*, pages 6028–6039. PMLR, 2020. [1](#), [2](#), [3](#), [4](#), [5](#), [6](#), [7](#), [8](#)
- [26] Tsung-Yi Lin, Priya Goyal, Ross Girshick, Kaiming He, and Piotr Dollár. Focal loss for dense object detection. In *Proceedings of the IEEE international conference on computer vision*, pages 2980–2988, 2017. [5](#)
- [27] Weitang Liu, Xiaoyun Wang, John Owens, and Yixuan Li. Energy-based out-of-distribution detection. *Advances in Neural Information Processing Systems*, 33:21464–21475, 2020. [1](#)
- [28] Mingsheng Long, Yue Cao, Jianmin Wang, and Michael Jordan. Learning transferable features with deep adaptation networks. In *International conference on machine learning*, pages 97–105. PMLR, 2015. [2](#)
- [29] Mingsheng Long, Zhangjie Cao, Jianmin Wang, and Michael I Jordan. Conditional adversarial domain adaptation. In *Proceedings of the 32nd International Conference on Neural Information Processing Systems*, pages 1647–1657, 2018. [2](#)
- [30] Mingsheng Long, Han Zhu, Jianmin Wang, and Michael I Jordan. Deep transfer learning with joint adaptation networks. In *International conference on machine learning*, pages 2208–2217. PMLR, 2017. [2](#)
- [31] Xingchao Peng, Ben Usman, Neela Kaushik, Judy Hoffman, Dequan Wang, and Kate Saenko. Visda: The visual domain adaptation challenge. *arXiv preprint arXiv:1710.06924*, 2017. [6](#)
- [32] Viraj Prabhu and Arjun Chandrasekaran. Active domain adaptation via clustering uncertainty-weighted embeddings. In *ICCV*, pages 8485–8494. IEEE, 2021. [1](#), [2](#), [3](#), [4](#), [6](#), [7](#)
- [33] Zhen Qiu, Yifan Zhang, Hongbin Lin, Shuaicheng Niu, Yanxia Liu, Qing Du, and Mingkui Tan. Source-free domain adaptation via avatar prototype generation and adaptation. *arXiv preprint arXiv:2106.15326*, 2021. [3](#), [6](#), [7](#)
- [34] Hiranmayi Ranganathan, Hemant Venkateswara, Shayok Chakraborty, and Sethuraman Panchanathan. Deep active learning for image classification. In *2017 IEEE International Conference on Image Processing (ICIP)*, pages 3934–3938. IEEE, 2017. [2](#)
- [35] Kate Saenko, Brian Kulis, Mario Fritz, and Trevor Darrell. Adapting visual category models to new domains. In *European conference on computer vision*, pages 213–226. Springer, 2010. [6](#)
- [36] Ozan Sener. Active learning for convolutional neural networks: A core-set approach. In *6th International Conference on Learning Representations, ICLR 2018, Vancouver, BC, Canada, April 30 - May 3, 2018, Conference Track Proceedings*. OpenReview.net, 2018. [2](#), [3](#), [6](#), [7](#)
- [37] Yuan Shi and Fei Sha. Information-theoretical learning of discriminative clusters for unsupervised domain adaptation. In *ICML*, 2012. [5](#)
- [38] Anurag Singh, Naren Doraiswamy, Sawa Takamuku, Megh Bhalerao, Titir Dutta, Soma Biswas, Aditya Chepuri, Balasubramanian Vengatesan, and Naotake Natori. Improving semi-supervised domain adaptation using effective target selection and semantics. In *IEEE Conference on Computer Vision and Pattern Recognition Workshops, CVPR Workshops 2021, virtual, June 19-25, 2021*, pages 2709–2718. Computer Vision Foundation / IEEE, 2021. [2](#), [4](#)
- [39] Serban Stan and Mohammad Rostami. Privacy preserving domain adaptation for semantic segmentation of medical images. *arXiv preprint arXiv:2101.00522*, 2021. [1](#)
- [40] Jong-Chyi Su, Yi-Hsuan Tsai, Kihyuk Sohn, Buyu Liu, Subhransu Maji, and Manmohan Chandraker. Active adversarial domain adaptation. In *IEEE Winter Conference on Applications of Computer Vision, WACV 2020, Snowmass Village, CO, USA, March 1-5, 2020*, pages 728–737. IEEE, 2020. [2](#), [3](#), [6](#), [7](#)
- [41] Hui Tang, Ke Chen, and Kui Jia. Unsupervised domain adaptation via structurally regularized deep clustering. In *Proceedings of the IEEE/CVF Conference on Computer Vision and Pattern Recognition (CVPR)*, June 2020. [5](#)
- [42] Takeshi Teshima, Issei Sato, and Masashi Sugiyama. Few-shot domain adaptation by causal mechanism transfer. In *International Conference on Machine Learning*, pages 9458–9469. PMLR, 2020. [2](#)
- [43] Chandra Thapa and Seyit Camtepe. Precision health data: Requirements, challenges and existing techniques for data security and privacy. *Computers in biology and medicine*, 129:104130, 2021. [1](#)
- [44] Qing Tian, Chuang Ma, Feng-Yuan Zhang, Shun Peng, and Hui Xue. Source-free unsupervised domain adaptation with sample transport learning. *J. Comput. Sci. Technol.*, 36(3):606–616, 2021. [2](#), [3](#)
- [45] Hemant Venkateswara, Jose Eusebio, Shayok Chakraborty, and Sethuraman Panchanathan. Deep hashing network for unsupervised domain adaptation. In *Proceedings of the IEEE conference on computer vision and pattern recognition*, pages 5018–5027, 2017. [1](#), [6](#)
- [46] Dan Wang and Yi Shang. A new active labeling method for deep learning. In *2014 International Joint Conference on Neural Networks, IJCNN 2014, Beijing, China, July 6-11, 2014*, pages 112–119. IEEE, 2014. [3](#), [6](#), [7](#), [8](#)
- [47] Jian Wang, Yongcheng Luo, Yan Zhao, and Jiabin Le. A survey on privacy preserving data mining. In *2009 First International Workshop on Database Technology and Applications*, pages 111–114. IEEE, 2009. [1](#)
- [48] Qi Wei, Lei Feng, Haoliang Sun, Ren Wang, Chenhui Guo, and Yilong Yin. Fine-grained classification with noisy labels. *arXiv preprint arXiv:2303.02404*, 2023. [5](#)
- [49] Qi Wei, Haoliang Sun, Xiankai Lu, and Yilong Yin. Self-filtering: A noise-aware sample selection for label noise with confidence penalization. In *Computer Vision—ECCV 2022: 17th European Conference, Tel Aviv, Israel, October 23–27, 2022, Proceedings, Part XXX*, pages 516–532. Springer, 2022. [5](#)

- [50] Haifeng Xia, Handong Zhao, and Zhengming Ding. Adaptive adversarial network for source-free domain adaptation. In *Proceedings of the IEEE/CVF International Conference on Computer Vision*, pages 9010–9019, 2021. 1, 3, 6, 7
- [51] Binhui Xie, Longhui Yuan, Shuang Li, Chi Harold Liu, Xinjing Cheng, and Guoren Wang. Active learning for domain adaptation: An energy-based approach. In *AAAI*, volume 36, pages 8708–8716, 2022. 2, 3, 6, 7
- [52] Guanglei Yang, Hao Tang, Zhun Zhong, Mingli Ding, Ling Shao, Nicu Sebe, and Elisa Ricci. Transformer-based source-free domain adaptation. *CoRR*, abs/2105.14138, 2021. 1
- [53] Shiqi Yang, Joost van de Weijer, Luis Herranz, Shangling Jui, et al. Exploiting the intrinsic neighborhood structure for source-free domain adaptation. *Advances in Neural Information Processing Systems*, 34, 2021. 3, 4, 5, 6, 7
- [54] Shiqi Yang, Yaxing Wang, Joost van de Weijer, Luis Herranz, and Shangling Jui. Generalized source-free domain adaptation. In *Proceedings of the IEEE/CVF International Conference on Computer Vision*, pages 8978–8987, 2021. 4
- [55] Zhi-Hua Zhou. *Machine learning*. Springer Nature, 2021. 4